Université Abou Moumouni-Niamey

Doctoral Research Program on Climate Change and Energy

(DRP-CCE)

Republic of Niger

INTERNATIONAL MASTER PROGRAM

IN RENEWABLE ENERGY AND GREEN HYDROGEN

SPECIALITY: PHOTOVOLTAICS FOR GREEN HYDROGEN TECHNOLOGY

MASTER THESIS

Topic:

ENERGY RETURN OF INVESTMENT (EROI) ANALYSIS OF DIRECTLY-COUPLED PHOTOVOLTAIC STORAGE SYSTEMS

Presented on the 27 September 2023

by: **Fatou K. SAINE**

Exam committee members

Chair: Prof. Madougou Saidou, University of Abdou Moumouni-Niger

Examinator: Dr. Inoussa Abdou Saley, University of Abdou Moumouni-Niger

Main Supervisors: Dr. Tsvetelina Merdzhanova, Forschungszentrum Jülich-Germany

Dr. Oleksandr Astakhov, Forschungszentrum Jülich-Germany

Local Supervisors: Prof. Rabani Adamou, University of Abdou Moumouni-Niger

Dr. Bonkaney Abdou Latif, University of Abdou Moumouni-Niger

Academic year 2022-2023

ACKNOWLEGEMENTS

I would like to express my profound gratitude to all those who helped me in one way or the other in pursuing my master's degree and conducting my research work.

First and foremost, I am deeply grateful to the Federal Ministry of Education and Research (BMBF), especially Prof Rovekamp, and the West African Science Service Centre on Climate Change and Adapted Land Use (WASCAL), for granting me the scholarship to pursue my master's degree.

I would like to thank the Director of the Institute of Photovoltaics and Climate Research (IEK5), Prof. Rau Uwe, his team, and administration at the Forschungszentrum Jülich (FZJ), in Germany for their immense support during the research work at the center.

I would like to also express my sincere gratitude to my supervisors at the Forschungszentrum Jülich (FZJ), Dr. Tsvetelina Merdzhanova, and Dr. Oleksandr Astakhov for sharing their scientific know how and guidance during this thesis work. Without their cooperation and insightful suggestions, completing this research work would have almost been impossible. My special thanks to Dr. Oleksandr Astakhov for the many brainstorming sessions, ingenious suggestions and time, which aided in shaping this work to scientific standards.

A Special thanks to my supervisors at the Abdou Moumouni University in Niger, Prof. Rabani Adamou, the WASCAL director for the Doctoral Research Program on climate change and energy, for his insightful feedbacks, and valuable advice. And Dr. Bonkaney Abdou Latif for his advice, helpful suggestions and feedbacks in improving my work.

I would also like to thank Dr. Ayouba, the coordinator of the Green Hydrogen program in Niger for his keen interest and advice.

My special thanks to the members of the photovoltaic and electrochemical devices in IEK5, for their support and motivation during the research work.

Finally, I am sincerely thankful to my family and friends for their unwavering support and belief in me that kept me motivated throughout this journey and which significantly contributed to the development of this work. I am especially grateful to my parents for their continuous and incomparable love, help and support.

ABSTRACT

To address the energy dependence challenges and the climate change issues, Hydrogen has received unprecedented attention, as an energy carrier and a storage medium. In this research work, a quasi-island utility scale of 1MW Photovoltaic storage system that meets the energy requirements of the water electrolysis process for the generation of Hydrogen, under the climatic condition of Farafenni town, in The Gambia was designed as a reference case. The energetic performance of three different system configurations, the reference case scenario, direct coupled photovoltaic-electrochemical water splitting system, and the battery assisted direct coupled photovoltaic-electrochemical system were analysed using the Energy Return of Investment metric. The Life cycle assessment method and the System Advisory Model simulation tool were used for the analysis and the results imply that for the configuration to operate without grid inter-connection, a battery capacity of 3MWh will be required. The net energy analysis metric results are 2.36, 2.48, and 2.39 for the reference case, the direct coupled Photovoltaic-electrochemical water splitting system, and the battery assisted direct coupled photovoltaic-electrochemical system, respectively. These values indicate that the direct-coupled photovoltaic storage systems are viable options for hydrogen production.

KEYWORDS: Energy return of investment; Renewable energies; Photovoltaic technologies; Electrochemical-water system; Lithium-ion Batteries.

RÉSUMÉ

Pour répondre aux défis de la dépendance énergétique et aux enjeux du changement climatique, l'hydrogène a fait l'objet d'une attention sans précédent, en tant que vecteur énergétique et support de stockage. Dans ce travail de recherche, un système de stockage photovoltaïque quasi-insulaire de 1 MW répondant aux besoins énergétiques du processus d'électrolyse de l'eau pour la production d'hydrogène, dans les conditions climatiques de la ville de Farafenni, en Gambie, a été conçu comme cas de référence. Les performances énergétiques de trois configurations de système différentes, le scénario de référence, le système de séparation de l'eau photovoltaïque-électrochimique à couplage direct et le système photovoltaïque-électrochimique à couplage direct assisté par batterie ont été analysées à l'aide de la mesure du retour sur investissement énergétique. La méthode d'évaluation du cycle de vie et l'outil de simulation System Advisory Model a été utilisés pour l'analyse et les résultats impliquent que pour que la configuration fonctionne sans interconnexion au réseau, une capacité de batterie de 3 MWh sera nécessaire. Les résultats métriques de l'analyse de l'énergie nette sont respectivement de 2,36, 2,48 et 2,39 pour le cas de référence, le système de séparation de l'eau photovoltaïque-électrochimique à couplage direct et le système photovoltaïque-électrochimique à couplage direct assisté par batterie. Ces valeurs indiquent que les systèmes de stockage photovoltaïques à couplage direct sont des options viables pour la production d'hydrogène.

MOTS-CLÉS: Retour énergétique de l'investissement; Énergies renouvelables; Technologies photovoltaïques; Système électrochimique à base d'eau; Batteries lithium-ion.

ACRONYMS AND ABBREVIATIONS

AC	**:**	Alternating Current
AWE	**:**	Alkaline water electrolysis
BOS	**:**	Balance of system
DC	**:**	Direct Current
DOD	**:**	Depth of discharge
EC	**:**	Electrochemical water splitting system
EPBT	**:**	Energy payback time
EU	**:**	European Union
EROI	**:**	Energy return of investment
IEA-PVPS	**:**	International Energy Agency-Photovoltaic power system programme
H2	**:**	Hydrogen
I-V	**:**	Current-Voltage
KOH	**:**	Potassium-hydroxide
MPP	**:**	Maximum Power Point
MPPT	**:**	Maximum Power Point Tracking
NaOH	**:**	Sodium-hydroxide
NREL	**:**	National renewable energy laboratory
NSRDB	**:**	National-Solar Radiation database
PEM	**:**	Polymer-electrolyte membrane water electrolysis
PV	**:**	Solar Photovoltaic
PV-EC	**:**	Photovoltaic-electrochemical water splitting system
PV-EC-B	**:**	Photovoltaic-electrochemical water splitting-Battery system
SAM	**:**	System Advisory Model
SOEC	**:**	Solid Oxide electrolysis cell
LCI	**:**	Life-cycle inventory

List of Figures

Figure 2.1. *Single-diode model* 10
Figure 2.2. *Schematic diagram of a DC-AC-DC configuration setup* 11
Figure 2.3. *Schematic diagram of the main components of green hydrogen production facility that include battery storage* 12
Figure 2.4. *Principle structure of commercial AWEs (bipolar form)* 14
Figure 2.5. *Map of the Gambia* 18
Figure 2.6. *Boundary condition of the EROI metric* 23

Figure 3.1. *Sketch of the Reference system configuration* 27
Figure 3.2. *Unpredicted and the predicted EC load profiles with the PV generation of the system* 28
Figure 3. 3. *Schematic representation of the EC operating conditions* 29
Figure 3. 4. *Lifetime energy required as battery capacity varies for the Unpredicted, daily and hourly predicted EC load profile* 31
Figure 3.5. *Lifetime energy required as EC minimum power varies for the daily and hourly prediction* 31
Figure 3.6. *Schematic representation of the direct coupled PV-EC configuration* 34
Figure 3.7. *Schematic representation of the direct coupled PV-EC-B configuration* 35

List of Tables

Table 3.1. *Components of the system and their total embodied energy for the construction and operation of the system* 32
Table 3.2. *Total embodied energy in the reference-case configuration* 33
Table 3.3. *Total embedded energy in the direct coupled PV-EC configuration* 34
Table 3.4. Total embedded energy in the direct coupled PV-EC-B configuration 35
Table 3.5. *System's total embedded energy, EPBT and EROI* 36

Table of Contents

ACKNOWLEGEMENTS i
ABSTRACT ii
RÉSUMÉ iii
List of Figures v
List of Tables vi
Table of Contents vii
INTRODUCTION 1
Problem Statement 3
Research Questions 3
Research Hypotheses 3
Research Objectives 4
General Objective 4
Specific Objectives 4
CHAPTER 1: LITERATURE REVIEW 5
1.1. EROI Analysis of Photovoltaic Technologies 5
1.2. EROI Analysis of Electrolyser-Technologies 7
CHAPTER 2: MATERIALS, METHODS AND DATA PROCESSING 9
2.1. System Descriptions 9
2.2. Components of the System and Their Architectures 9
2.2.1. PV Array and the possible Inter-Connection or Configurations of the Systems 9
2.2.2. Alkaline Electrolyser 12
2.2.3. Lithium-Ion Battery 16
2.3. Study Area 17
2.4. Data Collection 19
2.5. Simulating PV Systems with Storage 19
2.6. EROI Computation 21
2.6.1. Embedded Primary Energy 24
CHAPTER 3: RESULTS AND DISCUSSION 26
3.1. System Requirements/Presentation 26
3.2. System Sizing and Design 26

3.3. System Optimization 27
3.3.1. Unpredicted and Predicted EC Load Profile 28
3.3.2. Parameters used for System Optimization 29
3.4. Embodied Energy 32
3.4.1. Embedded Energy of the Reference Case Configuration 33
3.4.2. Embedded Energy of the Direct-Coupled Systems 33
3.5. Comparisons of the Different Configurations 36
CONCLUSION AND PERSPECTIVES 38
REFERENCES 39

INTRODUCTION

The global primary energy demand is high and is expected to rise by 1.3% each year until 2040 (Megía et al., 2021) due to economic growth, increase in population and advances in technology. Majority of the energy production comes from fossil fuels such as oil, natural gas, and coal resulting in the emission of greenhouse gases (i.e., carbon dioxide, nitrogen oxides, and other volatile compounds, and solid particles) in the atmosphere which significantly contribute to the global climate change. Therefore, in order to limit the global average temperature increase to 1.5 ^{0}C which is in line with the Paris agreement of reaching global net zero emissions by 2050 and achieve carbon neutrality, an urgent need to move towards alternative sources of energy is required (Megía et al., 2021; Umair & IEEE, 2023).

The most recognized and promising clean energy carrier, and long-term storage medium in the 21st century is hydrogen energy (i.e., hydrogen produced from water electrolysis with the supply of renewable energies), because of its advantages of high energy density, easy storage, and zero carbon emission (Gu et al., 2023). However, due to intermittent nature of renewables, backup power and energy storage technologies are required. And Solar-driven water electrolysis is cosidered, a promising way to convert light energy to chemical energy in the form of Hydrogen gas. This implies that conversion of the excess renewable generation such as solar photovoltaic (PV) energy into hydrogen and storing the green energy in chemical form, is the way forward (Guangling Zhao et al., 2020; Kin et al., 2022).

Recently, the share of renewable energy in the power market has boosted and among this renewable energies, Photovoltaic (PV) generation is the most popular large-scale green power generation route (Gu et al., 2023), with cumulative global PV-installation of about 850 GW at the end of 2021 (Fraunhofer Institute for Solar Energy Systems, 2023). Photovoltaic (PV) generation is also one of the best sources of renewable energy (Umair & IEEE, 2023).

According to (Fraunhofer Institute for Solar Energy Systems, 2023), for the last 24 years, the energy payback time (EPBT) of photovoltaic systems, reduces by 12.8%, each time the cumulative production doubled. And under the trend of increasing deployment and decreasing manufactural costs of renewable energies, solar module prices has also decrease by 25% from the last 40 years with each doubling of the cumulated global module production. This reduction in price is due to technological improvements, and economics of scale. For instance, the cost of a typical 10 to 100

kWp PV rooftop system in Germany in 1990 was around 14,000 euro/kWp but by the end of 2020 such system just cost 7.4% of the price in 1990 which results in a net-price regression of about 92% over a period of 30 years (Fraunhofer Institute for Solar Energy Systems, 2023).

Renewable energy installation required energy storage technologies to reduce intermittency, smoothen output, and improve controllability. Among the photovoltaic-storage systems, batteries are the most frequently used as short-term storage to stabilized the fluctuations because of their robustness and relatively low cost (Xiong & Nour, 2019). However, hydrogen produced by water electrolysis (i.e., electrochemical water splitting devices) with the supply of renewables such as photovoltaic energies can be used for seasonal storage (Wei et al., 2022)**.**

With the power production sector releasing the highest amount of carbon emissions of about 13,603 MT worldwide (Shriyan, 2020), the transition from the fossil fuel dominated power sector to the green energy producing renewable energy plants is required. Over the past 3-4 decades, huge technological advancement in renewable energy technologies has been taking place, through intensive research and diffusion of technologies. For instance, the European Union (EU) targets the deployment of 40GW of renewable hydrogen electrolysers by the end of 2030. Netherlands plans to use 3-4 GW wind energy for hydrogen production from North Sea by 2030, which may go up to 10 GW by 2040. And likewise, Australia is planning the development of up to 15 GW scale of solar and wind energy for hydrogen production (Shriyan, 2020). However, among the solar-water splitting approaches, Photovoltaic-electrochemical (PV-EC) process has shown the highest solar-to-hydrogen efficiency (STH) of over 30% in the lab and is considered the most appropriate way for commercialization in the near future (Kin et al., 2022).

The configurations of the photovoltaic-electrochemical (PV-EC) system can be directly or indirectly coupled. The directly couple method, reduces losses in the energy transfer process because it does not require auxiliary equipment such as DC/DC converters and maximum power point tracking (MPPT) devices. However, its higher requirements lie in the structural matching of the PV array and the electrolyser (Gu et al., 2023). Among the water electrolysis technologies, alkaline electrolyser is the most established and mature technology (Tripathi & Subramanian, 2022). Also, reports have shown that both PV and alkaline electrolyser have a decent learning curve over the past decades individually (Shriyan, 2020), but very less has been investigated or implemented on connecting it at large MW scale as well as performing its long-term net energy

analysis. This work intends to fill this gap by performing a net energy analysis of the EROI metric for a large scale directly-coupled Photovoltaic-Storage systems.

The outline of this document is arranged as follows: A review on the various literature of EROI is given in chapter 1, followed by system description and explanation of the employ methods or procedures in Chapter 2, then simulated results are analysed in chapter 3. And finally, the conclusion and perspectives drawn from the research work are presented.

Problem Statement

Solar powered water electrolysis is considered to be one of the pathways towards deep decarbonization, because hydrogen (H_2) is emerging as the possible solution to the intermittency that arises from diurnal and seasonal variation of renewable energies due to its energy storage and carrier ability. However, to commensurate the upscaling required for renewable hydrogen, address climate change, and energy dependence challenges. It is crucial that the energetic performance of renewable hydrogen technologies or different energy system configurations are well understood. Hence, this present study seeks to better understand the energetic performance of the direct-coupled photovoltaic-electrochemical water splitting systems.

Research Questions

1. What is the photovoltaic-electrochemical water splitting (PV-EC) system long term viability?
2. What is the energy balance of the systems?
3. Which stage is the most energy-intensive in the process chain?

Research Hypotheses

The photovoltaic-electrochemical water splitting (PV-EC) systems are viable options for green hydrogen production.

Research Objectives

General Objective

The main objective of this research is to assess the energy performances by evaluating and comparing the EROI of the reference system with power electronics (i.e., PV-Inverter-EC-B) and the direct coupled PV-EC-B systems.

Specific Objectives

1. To determine the annual and lifetime energy generation in the system.
2. To determine embodied energy for the production, manufacturing, and operation of each system.
3. To determine the energy payback time (EPTB) of each system.

CHAPTER 1: LITERATURE REVIEW

Introduction

The net energy analysis comprises of both Energy Return of Investment (EROI) and Energy Payback Time (EPBT) analysis. The EPBT gives the time or period it takes in years for a project to return the energy that was initially invested in its construction. It can also be defined as the ratio of energy investments to the hydrogen energy supplied per year (Tripathi & Subramanian, 2022). On the other hand, the metric EROI which is the focus of this study captures the extent to which useful energy is yielded from a system or process (Dumas et al., 2022). It can be defined as the ratio of the hydrogen produced to the life cycle energy investments, including construction, maintenance, operation, and decommissioning of the plant (Tripathi & Subramanian, 2022). This means that the lower the EROI of an energy source, the more input energy is required to produce an output energy (Dumas et al., 2022).

The EROI analysis can also be viewed as a subset of the Life cycle assessment (LCA), which is a methodology for estimating the emissions of products during a system or product whole service lifetime, from raw material extraction and refinement, to manufacturing processes, usage, transports and disposal (Barbera E et al., 2022). LCA method involves the definition of the goal and scope of the study, and Life Cycle Inventory (LCI) (i.e., the collection of material and energy balances over the entire life cycle of the product system). And these are the 2 guidelines in the LCA analyses (ISO 14040) methodology recommended by the IEEE to be clearly stated with the conventions outlined by the IEA PV Systems Programme Task 12 when conducting the EROI analysis (Carbajales-Dale et al., 2015).

In this chapter, the main findings from researchers in the domain or thematic is discussed.

1.1. EROI Analysis of Photovoltaic Technologies

(Bhandari et al., 2015) carried out a systematic review and a meta-analysis of the embedded energy, energy payback time (EPBT), and EROI metrics of PV technologies, published in the period of 2000-2013. Their study implies that the mean harmonized EPBT ranges from 1.0 to 4.1 years from lowest to highest with module types ranked in the following order; Cadmium telluride (CdTe), Copper indium gallium diselenide (CIGS), Amorphous silicon (a:Si), Polycrystalline

silicon (Poly-Si) and Monocrystalline silicon (mono-Si). And the mean harmonized EROI range from 8.7 to 34.2. The study concluded that across the different types of PV technologies, the variation in embedded energy was greater than the variation in efficiency and performance ratio.

In (Koppelaar's, 2017) review, he reproduced and harmonized 34 studies, for solar-PV energy payback time (EPBT) and energy return of investment (EROI). The results show that the mean harmonized solar PV's EPBT and EROI may be less or half when old data sets are used as compared to recent data sets due to technological improvements. In his analysis data age correction was done and he obtained a mean harmonized EROI of 9.7 and 11.4 for mono and polysilicon solar-PV respectively This argument was well proved by the recent study of Tripathi and Subramanian in Indian conditions. The study performed a net energy analysis for a solar generation system and the results obtained are 1.84 years for the energy payback time and 12.56 for the EROI (Tripathi & Subramanian, 2022).

On the other hand (Kurland & Benson, 2019), quantifies how an addition of a lithium-ion (Li-ion) battery affects the energetic performance of a typical residential photovoltaic (PV) system when either the power generated is self-consumed or made available to the distribution grid for a wide range of climatic conditions of 5 different locations in U.S.A. The results showed an energy return of investment (EROI) between 14 and 27 for the PV-system without storage (i.e., when the excess power generated is made available to the customers of the power grid), the addition of a 12 kWh Li-ion battery to this system, decreases the EROI by 21%, and doubling the battery size decreases EROI by 34% (i.e., EROI value ranges from approximately 9.24 to 17.82) compared to the case without a battery. This decrement in EROI can be attributed to the energy-intensive manufacturing of batteries and losses associated with the round-trip efficiency of charge/discharge cycles.

However, in the situation where all excess power generation is curtailed and not sent to the grid or stored, their results show a systems EROI drops that ranges from 7 to 14. The addition of a 12kWh battery to avoid this curtailment increases the EROI to about 12 and 42% but this EROI is still lower than in the cases where the system is providing the excess power to the grid. And doubling the battery capacity decreases the total system EROI to an extent similar to the case where the system is curtailing all excess generation. According to these results, a battery can increase EROI of a PV system in cases where excess generation is curtailed or cannot be fed into the grid.

However, it can never reach the same levels as a system with the potential to export power to the grid, and oversizing the battery can end up eating all the gain obtained in the total EROI (Davidsson Kurland & Benson, 2019)**.**

Similarly, (Müller & Chartouni, 2022) did an analysis by investigating the aspect of sustainability in residential PV installations combined with batteries, with a focus on EROI and CO2 reduction potential. Special attention was paid to the situations where an excess energy generated from photovoltaic power is not allowed to be fully fed into the distribution grid and has to be (partly) curtailed. In this analysis, three different European countries: Switzerland, Norway, and Spain were chosen to estimate the impact of residential solar batteries. The combined EROI of PV coupled with a battery was shown to be greater for all battery sizes up to 30 kWh compared to a scenario where excess PV production would be curtailed, with Spain's EROI almost doubling from around 8 for the case of no battery to 15 for an 18kWh battery. For Switzerland and Norway, the EROI improves by about 50% to 11 and 9, respectively, with the ideal size being smaller at 12 kWh. Also, his study shows that the last decade, energy intensities for the production of Li-ion batteries have decreased by over 30% when comparing data from the period of 2013 to 2020. This implies that, the impact of storage on EROI depends on the quantities and types of storage adopted and their operational strategies (Diesendorf & Wiedmann, 2020).

1.2. EROI Analysis of Electrolyser-Technologies

Hydrogen can be produced through electrolysis by using either an off-grid or an on-grid configuration. The off-grid configuration also known as the island or co-located setup, only utilize the energy produced by the on-site energy source and has no connection with the grid. In this configuration, the energy source is clearly identifiable, and the hydrogen produced can be easily classified as renewable, low-carbon, or generated by fossil fuels, based on the on-site power plant. The off-grid configuration is the simplest approach to ensure that the electricity used to produce hydrogen is 100 % renewable. However, it limits the operation of the electrolyser to the periods when renewable electricity can be produced or requires an additional storage device.

In the on-grid configuration, the electricity is sourced from the grid. Therefore, it becomes more difficult to ensure its renewable nature, because grid electricity is usually generated by a mix of renewable, nuclear and fossil sources (Gregor, 2023).

In this vain, (Palmer et al., 2021) studied the production of hydrogen using solar PV electrolysis and reported EPBT and EROI of 4.1 years and 4.6 for solar battery-based systems, and 3.7 years and 5.0 for solar grid-based systems with grid import.

Similarly, (Barbera et al., 2022) used process simulation to obtain material and energy balances for several hydrogen generation processes, each denoted by a unique colour code: (i) green hydrogen, produced by electrolysis of water using electricity from renewable sources, (ii) grid hydrogen, produced by electrolysis using grid electricity, (iii) grey hydrogen, produced from natural gas using steam reforming and (iv) blue hydrogen, like grey one, but coupled with carbon capture and storage. Their evaluations show that, the most sustainable hydrogen production method is the green hydrogen, produced by water electrolysis and the performance indicator, energy return of energy invested is 5.12 and 5.49 for green hydrogen and grid hydrogen respectively.

Also, (Tripathi & Subramanian, 2022) obtained results of EROI and EPBT for hydrogen production using Solar photovoltaic with polymer electrolyte membrane (PV-PEM), and Solar Photovoltaic with alkaline (PV-AWE) electrolysers. Their results are 7.7 years and 3.0, and 7.45 years and 3.11, respectively. This result implies that solar PV with PEM and AEC electrolysers are good indicator of energy return on energy investment (EROI) and are considered to be viable green hydrogen production methods.

CHAPTER 2: MATERIALS, METHODS AND DATA PROCESSING

Introduction

In this chapter, I describe the configurations of the systems and their components, and explicitly explain the Data and methodology adopted. First, by describing the System advisory model (SAM) simulation software tool, that is used for optimizing the system architecture and determining the lifetime energy output of the configurations, followed by the life cycle energy inventory analysis required for the computation of the EROI.

2.1. System Descriptions

EROI provide long-term performance analysis in real operating conditions and this is essential in direct coupled PV and storage systems, in order to ensure long term stability, robustness and reliability. Solar photovoltaics and water electrolysis are both well-established technologies, but there is little practical experience with them in terms of large-scale integrated systems (Palmer et al., 2021), especially direct coupled configurations. This is due to the distinct operational difficulties that arises in the off-grid solar powered electrolysis as compared to grid connected solar power (Palmer et al., 2021). In this analysis, a system configuration of 1 MW solar PV powered by electrolysis plant of 1 MW capacity to produce green hydrogen is considered. Three (3) scenarios are considered for comparison purpose (i.e., the reference case scenario, the direct-coupled Photovoltaic with electrochemical water splitting (PV-EC) system, and the battery assisted direct-coupled Photovoltaic electrochemical water splitting (PV-EC-B) system.

The reference-case scenario is the classical system of what exist in the market at the moment, it includes components such as: the PV array, inverter, Battery and electrochemical water splitting system. It is an indirect-couple configuration with more material composition than the direct-couple configurations.

2.2. Components of the System and Their Architectures

The three main components of the systems are the PV array, the alkaline electrolyser and the lithium-ion battery.

2.2.1. PV Array and the possible Inter-Connection or Configurations of the Systems

PV array is the assembly of PV module interconnected in series to form strings of required voltage which in turn are parallel connected with one or more inverters tying the whole array to a load or grid. Each PV module is made of solar cell-the basic PV component generating electricity from sunlight (Kosol Kiatreungwattana, Otto VanGeet, and Blaise Stoltenberg: NREL) and can be represented by the equivalent circuit model (Gutiérrez-Martín et al., 2021) or single diode model (Figure 2.1). This model consists of a parallel combination of a current source and a diode to represents a solar cell incorporated with a shunt and series resistances to consider manufacturing defects and contact resistance for practical applications. The current generated by the solar cell can be computed by Equation (1).

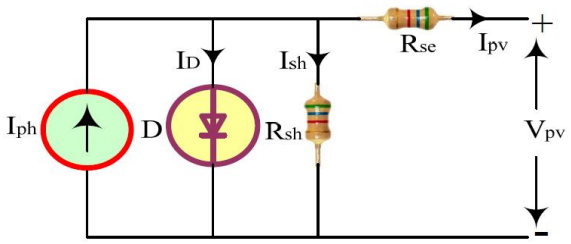

Figure 2.1. *Single-diode model* (Sharma et al., 2023)

$$I_{pv} = I_{ph} - I_D - I_{sh} \qquad (1)$$

And calculating the current through the diode and shunt resistor, can be done by using the Shockley equation and Ohm's law as shown in Equations (2) and (3), respectively.

$$I_D = I_0 \left[\exp\left(\frac{q}{N_{cs}KT}\left(V_{pv} + I_{pv}R_{se}\right)\right) - 1\right] \qquad (2)$$

$$I_{sh} = \frac{V_{pv} + I_{pv}R_{se}}{R_{sh}} \qquad (3)$$

Therefore, the distinctive Equation for the output current of solar cell can be written as:

$$I_{pv} = I_{Ph} - I_0 \left[\exp\left(\frac{q}{nN_{cs}KT}\left(V_{pv} + I_{pv}R_{se}\right)\right) - 1\right] - \frac{V_{pv} + I_{pv}R_{se}}{R_{sh}} \qquad (4)$$

Where I_{ph} is the current source which is in parallel with a single diode (i.e., photocurrent or light current), R_{sh} is the internal resistance, R_{se} is the series resistance, I_0 is the cell saturation current, T is the module temperature = 298 K, K is Boltzmann constant, q is elementary charge, N_{cs} is the number of cells in series and n is the cell ideality factor (Brauns & Turek, 2020).

There are various ways of connecting a PV array to an electrolyser to yield maximum output. This include both directly and indirectly (i.e., Power converter aided) coupling of the two components. The indirectly coupled method, architectures involve the use of auxiliary equipment or power electronics such as inverters, transformers, and rectifiers. This power electronics do not only increase the systems cost but also the amount of power loss in the conversion process. The direct coupled on the other hand can reduce the cost and also have higher efficiency provided that the structural matching of the PV array and the electrolyser are optimal (Gutiérrez-Martín et al., 2023). The state-of-the-art or usual configuration in the market today is indirectly coupled involving a PV array which is connected to an inverter (DC/AC) that converts the direct current (DC) to alternating current (AC) before feeding it to the electrolyser provided with a rectifier (Figure 2.2).

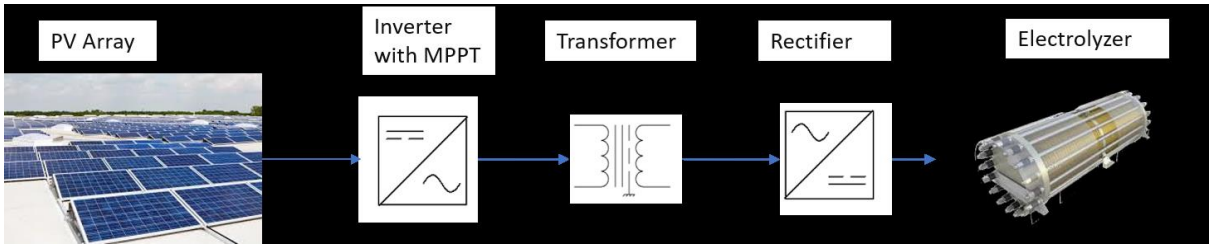

Figure 2.2. *Schematic diagram of a DC-AC-DC configuration setup* (Shriyan, 2020)

Another option is the coupling the PV array with an electrolyser, and a DC/DC (MPPT) converter to control the current and voltage of the PV modules, by extracting the maximum possible energy for any solar-load condition. This method is not yet standard solution in the sector but has lower costs and can achieve high efficiency as long as the coupling of output from PV and the electrolyser is optimal. It is considered that, these systems can be more competitive and should be developed for local solar H_2 production since they avoid the cost and energy loss of inverters, although their greatest difficulty lies in the fact that there are no generalizable topologies for the

projects as it happens with other DC technologies such as batteries (Gutiérrez-Martín et al., 2023) (Figure 2.3).

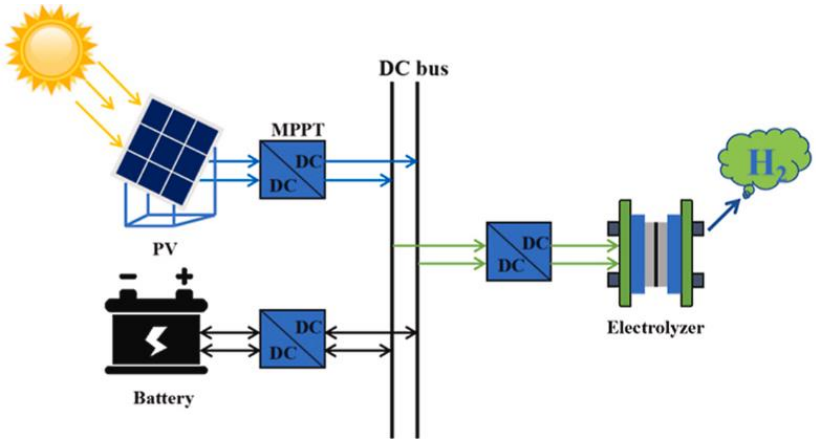

Figure 2.3. *Schematic diagram of the main components of green hydrogen production facility that include battery storage* (Gu et al., 2023)

The direct coupling of the PV array and an electrolyser is the simplest connection since it does not require any power electronics but requires a proper initial design to avoid energy losses. The operating point of this configuration is simply the intersections of the PV and electrolyser curves. However, this connection can result to power losses over time with respect to optimal Maximum Power Point Tracking (MPPT) and reduce flexibility of design (sizing) since the voltage range of electrolyser should be compatible with the possible PV voltages (Gutiérrez-Martín et al., 2023).

2.2.2. Alkaline Electrolyser

Water electrolysis is one of the most effective methods of hydrogen production because it splits water molecules and only generates pure oxygen as by-product while utilizing direct current (DC) derived from renewable sources such as solar energy (Frank et al., 2022; Tripathi & Subramanian, 2022). Water electrolysers are also categorized into three main technologies (i.e., alkaline water electrolysis (AWE), proton exchange membrane water electrolysis (PEM), and solid oxide electrolysis cells (SOEC). All the three types of electrolysers are already under commercialization, but even within the same category some concepts are more mature than others: for example, large-scale atmospheric alkaline water electrochemical cell (AWE) date back to the start of the twentieth

century, whereas designs tailored to pressurized operation only became common in the second half of the twentieth century (Ehlers et al., 2023).

SOEC enables water electrolysis at high temperatures of about 600–900 °C, with an efficiency higher than the PEM electrolysers and AWE. However, its sealing issues, thermal stability of materials, and gas mixture challenges are hindering its practical applications. On the other hand, PEM electrolysers are more efficient and allow higher current densities than AWE. However, its main disadvantage is the high capital cost of the acid-tolerance components like the Nafion membrane, titanium bipolar plates, and novel metal catalysts. In addition, their shorter lifetimes as compared to AWE have also hindered their application in large-scale power-to-gas scenarios. In contrast, alkaline electrolysers' earth-abundant electrocatalysts are stable enough to run both half-reactions, and their lifetime can reach up to 15 years. Therefore, alkaline electrolysers are suitable for large-scale electrolytic hydrogen projects (Xia et al., 2023).

It is also worth noting that some of the limitations commonly ascribed to alkaline water electrolysers such as low current densities and inability to operate with intermittent renewable energy sources originate in now-outdated atmospheric electrolysers originally designed for continuous operation in industrial sites with access to inexpensive electricity (e.g., hydroelectric power). Currently, with the state-of-the-art pressurized alkaline electrolysers can achieve performance and flexibility figures that are competitive with PEM while sidestepping material availability issues (Ehlers et al., 2023)**.**

Alkaline water electrolysis (AWE) consists of an anode and a cathode separated by a thin, porous ceramic diaphragm immersed in an alkaline electrolyte (Tripathi & Subramanian, 2022). The electrolyte is based on a liquid solution that may be potassium hydroxide (KOH) or sodium hydroxide (NaOH). However, manufacturers prefer to use KOH instead of NaOH since an aqueous solution with 25-30 wt.% KOH features a higher specific electrolyte conductivity at a standard temperature range from 50 to 80°C (Frank et al., 2022). The electrolytic cell, is the basic element of an alkaline electrolyser consisting of the bipolar plates, anode/cathode catalysts, and a diaphragm.

Commercially available alkaline water electrolysers are usually in bipolar form, and are composed of several cells connected in series. Under this condition, each electrode, except for the first and the last ones, has two polarities, the anode side and the cathode side, which belong to two

adjacent cells. In addition, the hydrogen channel, oxygen channel, and electrolyte channel are shared by all cells (Figure 2.4).

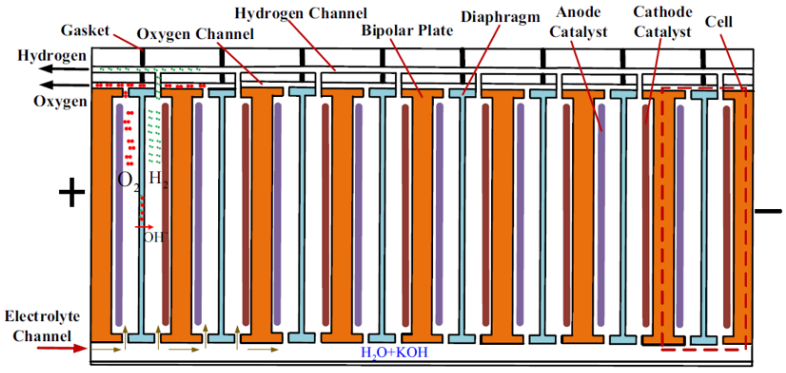

Figure 2.4. *Principle structure of commercial AWEs (bipolar form)* (Xia et al., 2023)

The behaviour of alkaline electrolysers can by describe by the following parameters:

- **The cell voltage:** which is the actual voltage that an electrolyser operates. It considers all the losses that occurs during operation in the electrolyser cell and can be determined using equation (5). It is simply the sum of the reversible voltage and all the overpotentials that occurs in the electrolyser;

$$V_{cell} = V_{rev} + V_{act} + V_{ohm} + V_{con} \qquad (5)$$

Where V_{rev} is reversible voltage, V_{act} is activation overvoltage, V_{ohm} is ohmic overvoltage, and V_{con} is concentration overvoltage.

- **The reversible cell voltage (V_{rev}):** which is the minimum voltage that is required for the electrolysis to take place. It is mathematically expressed as:

$$V_{rev} = \frac{\Delta G}{nF} \qquad (6)$$

Where G is the Gibbs energy, n is number of electron and F is Faraday's Constant. However, at standard condition (i.e., 25°C and 1 bar), the Gibbs energy for water splitting (G) is equals to 237. 2 kJ mol and Faraday's Constant equals to 96485 C mol, and the number of electron transfer for an alkaline electrolyser (n) = 2. Substituting these values in the equation yields V_{rev} = 1.229V.

- **Activation overvoltage:** is the overvoltage that is related to the extra energy required to start the oxygen and hydrogen formation process in the electrodes. It is expressed as:

$$V_{act} = slog\left(\frac{t_1 + \frac{t_2}{T} + \frac{t_3}{T^2}}{A} I + 1\right) \qquad (7)$$

Where s, t1, t2, t3 are the coefficient for overvoltage on electrodes, I is the current density, T is the temperature of the cell and A is the electrode area respectively.

- **Ohmic overvoltage:** is the overvoltage due to overall resistance of all components of the electrical circuit. These include cell elements such as electrodes, interconnection, and separating diaphragm to the electrons. If the distance between the anode and cathode is shorten, the overvoltage can be reduced (Frank et al., 2022).

$$V_{ohm} = \frac{r_1 + r_2 T}{A} I \qquad (8)$$

Where r_1 and r_2 are parameter related to ohmic resistance of electrolyte.

- **Concentration overvoltage:** is caused by mass transport processes (i.e., convection and diffusion). It occurs at very high current density approximately greater than 800 mA/cm^2 which is much higher than operating range of current density of an alkaline electrolyser also, the concentration overvoltage V_{con} is much lower than V_{act} and V_{ohm}. Therefore, in many cases, the effect of concentration or mass transfer overpotential are neglected (Niroula et al., 2023) for alkaline electrolysers, and the equation reduces to:

$$V_{cell} = V_{rev} + V_{act} + V_{ohmic} \qquad (9)$$

Therefore V; becomes

$$V_{cell} = \frac{\Delta G}{nF} + slog\left(\frac{t_1 + \frac{t_2}{T} + \frac{t_3}{T^2}}{A} I + 1\right) + \frac{r_1 + r_2 T}{A} I \qquad (10)$$

Which is known as the Oystein Ulleberg's equation (Brauns & Turek, 2020; Nkanga et al., 2021)**.**

In order to attain the operating point of a direct coupled PV modules and electrolyser.

The combination of the single diode model and the Ulberg's equation under varying solar irradiance and temperature is often used to obtain the intersection point of the I-V curves of the PV modules and the electrolyser. The coupling factor also called the coupling efficiency is the ratio of the power provided to the electrolyser to the maximum power point (MPP) of PV modules (Gutiérrez-Martín et al., 2021)**.**

2.2.3. Lithium-Ion Battery

Battery storage system are electrochemical devices that store excess energy in the form of electrochemical energy, inside the electrodes and electrolyte of the battery. Similar to electrolysers, the electrochemical losses in a battery can occur from the concentration overpotential, ohmic overpotential and activation overpotential. The most well-established battery technologies are lithium-ion batteries and lead-acid batteries. Lead-acid batteries offer a better option in terms of cost; however, their limited life-cycle means they must be replaced every 3 years. Therefore, the choice of technology for this research work is the lithium-ion battery since it offers the best option in terms of performance, life-cycle, and technological maturity. Lithium-ion batteries have high depth of discharge (DoD) of about 90-100% (Megan, 2020)**,** have fast response time and are maintenance free and abundant. They are also constantly improving in terms of energy density, power density, and cost with their efficiency slowly increasing and frequently reported to be between 93% and 95% (Schoehuijs, 2018)**.**

The lithium-ion cell which is capable of storing energy electrochemically consist of four major components (i.e., the positive electrode, separator, electrolyte, and negative electrode). When the battery is being charge or discharge, lithium ions are moved from one electrode to the other through the separator soaked with electrolyte which results in electrons circulating through the external circuit.

During the charging process, lithium ions are transported from the positive electrode or anode to the negative electrode or cathode. However, during the discharge process lithium ions are transported from the negative electrode or anode to the positive electrode or cathode. And when the cell is operating, redox reactions take place in both electrodes, thus delivering or consuming electrical energy when discharging or charging, respectively (Araoz, 2021).

The addition of battery in the direct-coupled system will help manage the balance of the components by compensating for the variability of PV outputs (Gutiérrez-Martín et al., 2023). In other words, the battery stabilizes the voltage and act as a buffer by getting charged when the production is more than the consumption rate, while getting discharged and providing current to the electrolyser when the PV-arrays current is not enough (Shcherbachenko et al., 2023). Although battery assisted electrolysis has the advantage of reducing the electrolyser size, it is convenient to operate it at part loads (i.e., PV array and electrolyser are larger) to grant H_2 production during the night (Astakhov et al., 2021; Gutiérrez-Martín et al., 2023; Kin et al., 2022).

2.3. Study Area

The location selected for this analysis is Farafenni town in the Gambia. The Gambia is located in the Sahelian zone of West Africa and is bordered by Senegal on its three sides, and the Atlantic Ocean coastline on its western edge. It is the smallest country on the continental Africa with a population of about 2,055,498 as of 2019 and a total land area of about 11,300km^2 (ESMAP, 2020). The river Gambia flows through the centre of the country from east to west, dividing it in two strips of land 25 to 50 km wide and about 300km long (*FAO, 2005)*.

The Gambia receives 2,500 sunshine hours per annum which translates to a solar irradiance of over 4.5 kW/m^2/day and has high solar radiation in all regions with average solar radiation at 4.4-6.7 kWh/m2/day. The climate condition of the country is characterized by two main seasons: a rainy season from June to October, and a longer dry season from November to May.

The periods of high insolation are between March and May when the diurnal variation between the minimum and maximum radiation values is small and the lowest radiation values are in December and January. Even during the rainy season, much of the country receives sufficient amounts of solar radiation at about 5 kWh/m2/day (IRENA, 2013).

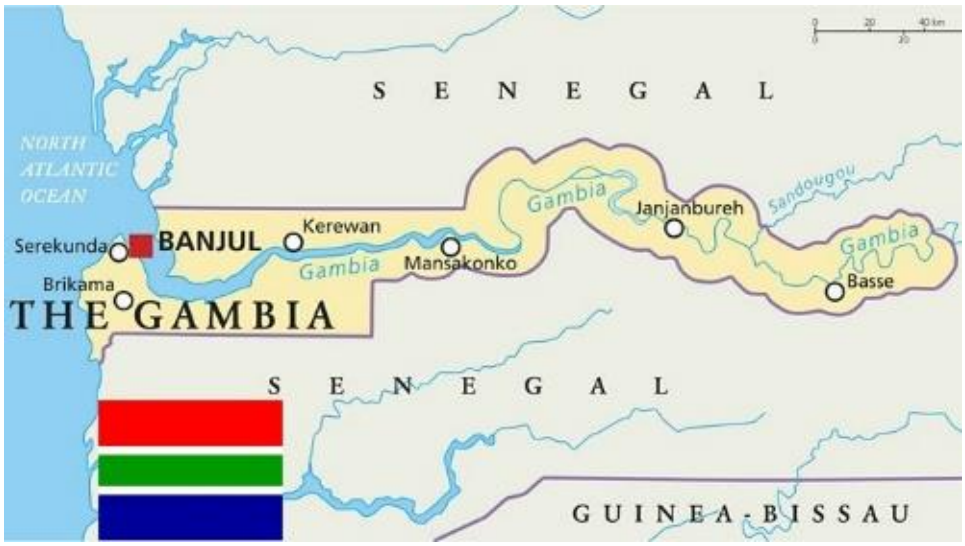

Figure 2.5. *Map of the Gambia* (Dr Y, 2021)

In the Gambia, electricity services are provided by the National Water and Electricity Company (NAWEC): a vertically integrated state-owned utility with 187,000 electricity customers by the end of 2017, of which more than 90 percent were in the Greater Banjul Area (i.e., Urban areas). The installed generation capacity in the country is 150 megawatts (MW), of which 139 MW of heavy fuel oil power plants are available in the Greater Banjul Area, but only 90 MW were available as of the end of December 2018 (World Bank, 2020).

Also, access to electricity has increased from about 25 percent of the population in 1996 to 47 percent in 2014. However, with significant and widening disparities in the acess of electricity between the rural and urban populations. For example, access to electricity increased in urban areas from 19 to 74 percent between 1996 and 2015 and decline in rural areas from 19 to 14 percent in the same period. So, in order to increase energy access in the rural areas, scale up generation capacity and for more efficient energy generation, and addition of renewable energy to the mix by studying and investing in solar photovoltaics and storage system is the way forward (World Bank, 2020).

2.4. Data Collection

The hourly weather data for Farafenni in the Gambia was collected from the National Solar Radiation Database (NSRDB) inbuilt in the System advisory model (SAM) and the unit energy data, required for the computation of the embedded or embodied energy in the components was obtained from the life-cycle inventory (LCI) in International Energy Agency Photovoltaic Power Systems programme (IEA PVPS 2020) database as well as in the literature. The LCI database was selected because it reflects up-to-date technological standards.

2.5. Simulating PV Systems with Storage

The constrain present by electrolysers in terms of operating condition, rises the need to optimized the system configurations to determine its performance under real operating conditions with changing irradiance and temperature before computation of the Energy return of investment (EROI). And this task was facilitated by the use of the system advisory model simulation software (SAM).

SAM is a tool developed by the U.S. Department of Energy's National Renewable Energy Laboratory (NREL), and is a techno-economic software model designed to facilitate decision making for people involved in the renewable energy industry, Project managers and engineers, financial and policy analysts, technology developers and researchers. This model was used because it has broad capabilities of analysing different renewable energies systems such as:

- Photovoltaic systems, from small residential rooftop to large utility-scale systems.
- Battery storage with Lithium ion, lead acid, or flow batteries for front-of-meter or behind-the-meter applications.
- Concentrating Solar Power systems for electric power generation, including parabolic trough, power tower, and linear Fresnel.
- Industrial process heat from parabolic trough and linear Fresnel systems.
- Wind power, from individual turbines to large wind farms.
- Marine energy wave and tidal systems.
- Solar water heating
- Fuel cells
- Geothermal power generation

- Biomass combustion for power generation and
- High concentration photovoltaic systems (Nate Blair, Nicholas DiOrio, Janine Freeman, Paul Gilman, Steven Janzou, Ty Neises, and Michael Wagner).

The detailed PV-battery model in the SAM simulation tool was used in this analysis because it allows detailed configuration of the PV field, inverter selection, battery and cell level specifications and dispatch.

The PV device selected for the analysis was the monocrystalline Trina solar vertex modules with 110 silicon cells. This module has a total surface area of 2.61m^2 and a rated power of 560Wp. Monocrystalline modules was selected because of their ability to withstand harsh weather condition with the lowest degradation rate (Gutiérrez-Martín et al., 2023)**.** Also, monocrystalline modules have higher efficiency as compared to multi-crystalline modules which can impact the energy generation of the system and with the continual improvement of solar modules, Price decrement is expected in the coming years.

The methodology employed for the performance evaluation was the energy management strategy which includes (Behmann et al., 2023; Vega-Garita et al., 2016):

- Forecasting: To estimate the power that needs to be exchanged in case of grid-connected systems. For this approach, an input of the temporal hourly resolution weather data of Farafenni in The Gambia and the required equipment's specification performance characteristics of the systems was used as input in the SAM Performance model, to make timestep-by-timestep calculations of a power system's electric output. Then, the amount of energy produced by the changing illumination conditions was used to forecast the consumption pattern of the electrolyser (EC).
- Optimization: This was done by forecasting or predicting for the day and hour ahead by changing the energy consumption pattern of the EC, in order to obtain better efficiencies and to get as much energy as possible to allow the battery to be fully charged in order to run the electrolyser no matter the outcome of the next day/hour.

Then, the simulation was run for the following three profiles:

- ✓ **Unpredicted EC profile:** In this method, a flat load profile was generated that assumed constant profile of the EC for hydrogen production throughout the whole year, regardless of whether it's a sunny or cloudy day.

- ✓ **Daily predicted EC profile:** Use PV generation to make a prediction of the EC profile by looking at a day ahead to determine the operating mode of the electrolyser before-hand.

- ✓ **Hourly predicted EC profile:** Use hourly prediction to determine the operating mode of the electrolyser.

2.6. EROI Computation

The life-cycle assessment method was used to compute the EROI metric, defined as the ratio of usable energy returned during a system's working life to the total energy required to make this energy usable as expressed in equation (11):

$$EROI = \frac{Energy\ output}{Energy\ input} \qquad (11)$$

This metric can be classified into three categories:

- ➢ **Standard or point of delivery EROI**: This takes into account the onsite and offsite energy investment to get the energy. It is simply defined as the ratio of the lifetime output energy of a system to the sum of the direct and indirect energy used to generate that output. The direct and indirect energy refers to both the on-site energy, and the energy required to manufacture the products used on-site. However, it does not include offsite energy such as energy associated with support labour, and financial services. It can be mathematically expressed as:

$$EROI_{st} = \frac{Energy\ returned\ to\ society}{Direct\ and\ Indirect\ Energy\ required\ to\ get\ that\ energy} \qquad (12)$$

- **Point of use EROI**: Involves the addition of the energy required for refinement and transportation (i.e., the energy cost to get and deliver the fuel). In this category, the boundaries are extended to include the costs associated with transporting the fuel to the point of use. This additional cost of energy will result in the reduction of the EROI.

$$EROI_{pou} = \frac{Energy\ returned\ to\ society}{Energy\ required\ to\ get\ and\ deliver\ that\ energy} \quad (13)$$

- **Extended EROI**: is the energy required to get, deliver and use a unit of the energy. This category on the other hand takes into account both the energy required to get and use a unit of the energy (Guerra-Martin, 2021)**.**

$$EROI_{ext} = \frac{Energy\ returned\ to\ society}{Energy\ required\ to\ get, deliver\ and\ use\ that\ energy} \quad (14)$$

In this study, the standard or point of deliver EROI is considered as the boundary condition for the analysis (Figure 2.6.) because of the aim is to analyse and compare the three (3) energy system configuration, as well as assess their long-term viability by considering its energy performance over the lifetime.

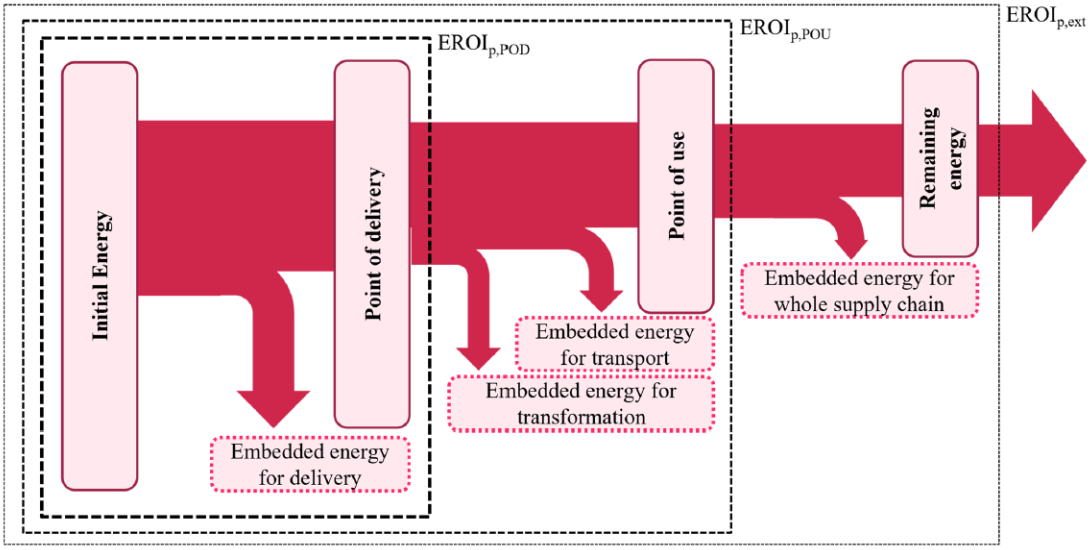

Figure 2.6. *Boundary condition of the EROI metric* (Pahud & Temmerman, 2022)

The EROI metric can also be defined using the EPBT indicator as expressed in equation 12:

$$EROI = \frac{Lifetime}{EPBT} \qquad (15)$$

And the EROI indicator EPBT can be defined with the following formular:

$$\mathrm{EPBT} = \frac{\mathrm{E_{INPUT}} + \mathrm{E_{BOS}}}{\mathrm{E_{OUTPUT\ ANNUALY}}} \qquad (16)$$

$$\mathrm{EPBT} = \frac{\text{Embedded Primary Energy}}{\text{Annual Energy Generated by system}} \qquad (17)$$

Where E_{INPUT} is the Primary energy input in the life cycle energy requirements which includes the energy required for manufacturing, installation, assembly, etc. E_{BOS} is the energy required for the balance of the system (BOS) and E_{OUTPUT} is the energy generated by the System.

This implies that the EROI ratio which is:

$$EROI = \frac{Lifetime\ Energy\ output}{Embedded\ Primary\ Energy} \quad (18)$$

can be expressed as:

$$EROI = \frac{Annual\ Energy\ output\ \times\ Lifetime}{Annual\ Energy\ Generated\ by\ System\ \times\ EPBT} \quad (19)$$

EROI is a dimensionless parameter that shows the amount of energy that is gained over the course of its entire lifetime. A higher EROI means that the energy generating system produces more energy and the system is deemed unviable if the EROI is less than 1:1. In industries, a minimum EROI of 3:1 is required. For a coupled PV-Electrolysis system, computation can be done using the following equations (Tripathi & Subramanian, 2022):

$$EPBT = \frac{Embedded\ Energy\ (Solar\ PV\ \&\ Electrolyzer)}{Annual\ hydrogen\ energy\ generation} \quad (20)$$

2.6.1. Embedded Primary Energy

The energy required for the construction, manufacturing, and assembly of a product or system was determine by computing all the unit energy required for the production of the raw materials, and manufacturing of the components in the system (such as the PV modules, inverters, and batteries). This computation was done by following the ISO14040, ISO14044, and International Energy Agency Photovoltaic Power Systems Programme Task 12 standards (IEAPVPS, T12), and transparently reporting the energy inputs for individual facili ties and non-module components, technology assumptions, and electric/thermal conversions was done as stated by (Koppelaar, 2017).

For the electrolyser, the scaling factor is used. Since material consumption and manufacturing energy of the balance of plant (BOP) and stack do not increase linearly as the plant size increases.

An appropriate scaling factor of 0.88 for the stack and 0.7 for the BOP is used as done by Tripathi and Subramanian. The life cycle energy analysis was assessed for the 1 MW facility using the equation of the scaling factor which is expressed as:

$$\frac{M_2}{M_1} = (P_2/P_1)^{\boldsymbol{b}} \qquad (21)$$

Where M_1 is the Material component 1 of the known weight, M_2 is the material component 2 of the unknown weight, P_1 is the capacity of the plant 1, and P_2 is the capacity of the plant 2.

CHAPTER 3: RESULTS AND DISCUSSION

Introduction

This chapter presents and discusses the results that were obtained as per the objectives of the study using the methods outline in the preceding chapter. The system requirement will be first defined for better understanding, followed by presentation, discussion, and comparison of the results.

3.1. System Requirements/Presentation

A 1MW PV capacity coupled with electrolyser system to operate in a quasi-island mode is proposed as the reference case in this work. In order words, the system attempts to minimize grid inter-connection and this operating mode is relevant in this scenario because of the low energy consumption in the Gambia, it is likely that the connection to the grid will be poorly maintained due to the weaknesses of the electric network. However, since researchers have found that the fluctuation of the Solar PV generation with power ramps and idle periods can cause degradation to water electrolysers. The system is assisted by Battery in order to smoothen PV power fluctuation and stabilize performance of the Electrochemical cell (Astakhov et al., 2021).

3.2. System Sizing and Design

To size the PV array for the reference case scenario, safety consideration according to regulations in-terms of maximum string voltage which is between 600-1500V as specified in the module datasheet (See appendix) was taken into consideration. An assumption of a maximum voltage of 1000V was used and the system configuration after sizing consists of 26 modules in a string and 69 strings in parallel. Figure 3.1 present the sketched of the reference system configuration. It consists of the PV- array, the electrochemical water splitting system (EC), the inverter and the Battery.

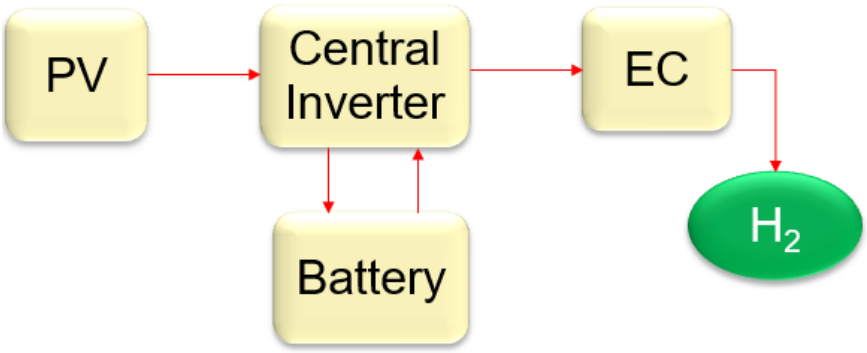

Figure 3.1. *Sketch of the Reference system configuration*

3.3. System Optimization

Due to the challenges that result from electrolysers (i.e., the time it take to respond to a change in power set-point and settle after a power set-point change, the rate at which they can change power consumption, the lower operation limit, or the minimum turndown level (Palmer et al., 2021), and the time they take to start up and shut down) there is need for storage device optimization to enable steady-state or continual operation of the electrolyser at lower operating limit.

For instance, alkaline electrolysers have a lower operating limit or require a minimal load of about 20 to 40% of the capacity and a system efficiency of 45 to 67% with an average of 63% as stated by (Mark Ruth, Ahmad Mayyas, and Margaret Mann). So, in order to attain the requirements for a steady-state operation of the electrolyser regardless of the intermittent nature of PV-array generation, it is important that the PV storage system is optimized for the system's self-consumption without grid-import and for better performance.

However, in this analysis, the reference system was optimized because it is the state-of-the-art configuration or classical system of what exist in the market with the availabe tools, and the three methods used for the optimization and the resulting graphs are presented in the proceeding sections.

3.3.1. Unpredicted and Predicted EC Load Profile

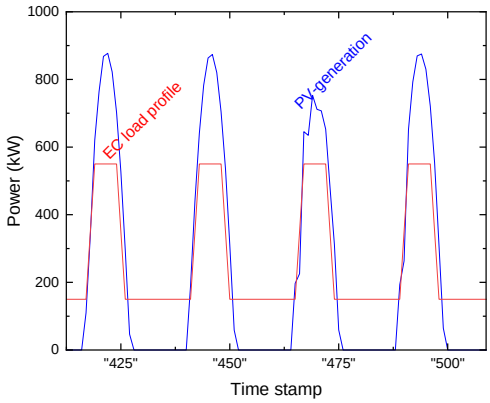

(a). *Unpredicted Ec load profile*

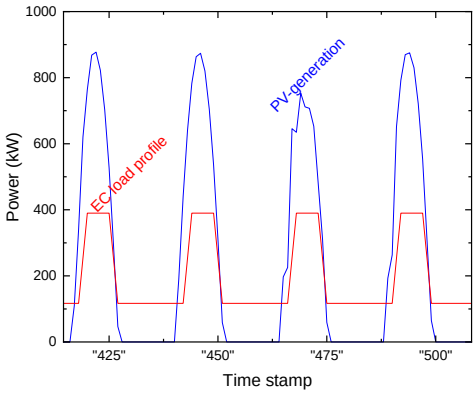

(b). *Daily-predicted Ec load profile*

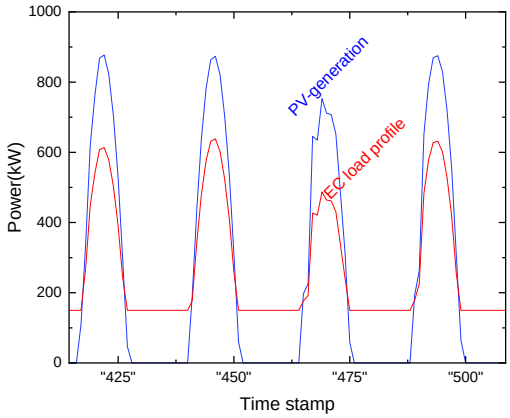

(c). *Hourly-predicted Ec load profile*

Figure 3.2. *Unpredicted and the predicted EC load profiles with the PV generation of the system*

Figure 3.2. presents the result of the unpredicted and predicted load profiles with PV-generation. In the unpredicted profile, the electrochemical water-splitting system (EC) was set to always operate at the nominal operating point of the electrolyser (i.e., assumed to be 50%) (Figure 3.2. (a)), and it is observed that for the optimum operation of the electrolyser during rainy and cloudy days for the production of hydrogen, an energy supplement will be required from the grid. However, to minimize the excess energy required by the system, and for more accurate prediction

of the EC load profile, the daily and hourly predicted profiles were generated in order to store maximum amount of energy in the battery that will allow the operation of the EC regardless of the pattern of the PV- generation.

In these predicted profiles (i.e., figure 3.2. (b) and (c)), it was observed that, more energy generation from the PV profile can be store in the battery to be used during cloudy and rainy days. However, more accurate prediction that follows the PV generation pattern was observed in the predicted hourly EC load profile.

3.3.2. Parameters used for System Optimization

Figure 3.3. presens the schematic representation of the operating condition of the electrolyser. It was observed that the minimal operating point of the electrolyser is the key factor for system optimization because of the lower operating limit or minimal power ranges of manufactured electrolysers (i.e., 20 to 40 % of the nominal operating power of the alkaline electrolyser as given by (Mark Ruth, Ahmad Mayyas, and Margaret Mann)). Hence, this result in huge amount of electricity or large storage medium requirenment for the operation of the electrolyzer when there is no PV generation. However, if new manufactured electrolyzers have operating limit lower than 20% of the nominal power, great improvements will be observed.

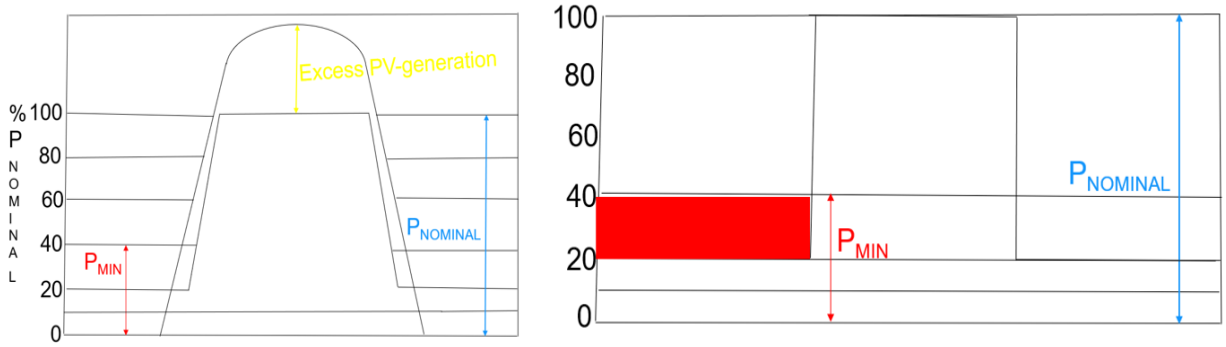

Figure 3. 3. *Schematic representation of the EC operating conditions*

Therefore, to optimize the system, two parameters were used. The excess PV generation that could be supplied to the grid and excess energy that would be required from the grid to run the electrolyser as battery capacity changes (i.e., energy to and from the grid), and the hydrogen production from the EC (i.e., the energy of the EC or the minimal power of the EC).

The graphs represented in Figure 3.4. presents, the grid interaction with the system as the battery capacity changes for the un-predicted and predicted load profiles of the EC respectively. The amount of energy supplied or required from the grid throughout the lifetime of the system was plotted. According to (Mark Ruth, Ahmad Mayyas, and Margaret Mann) the system lifetime of alkaline water electrolysis (AWE) is 20 to 30 years, so a system lifetime of 25 years was considered taking into account both the lifetime of the PV system and the AWE system.

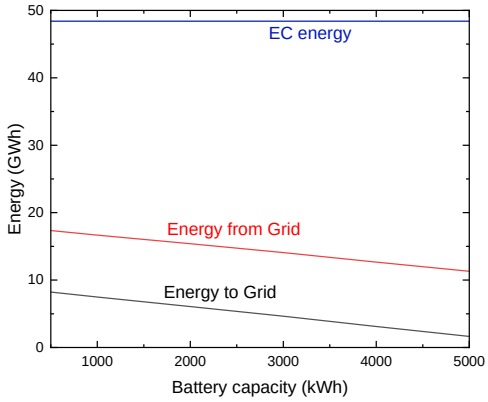

(a). *Unpredicted Ec load profile*

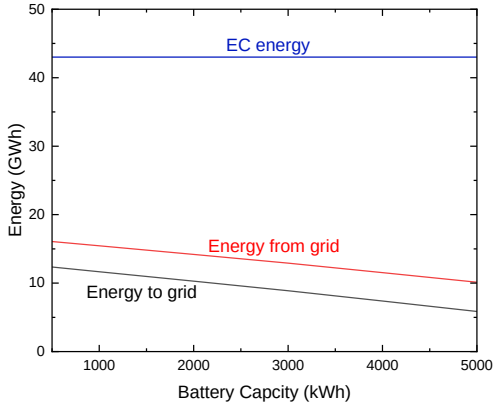

(b). *Daily predicted Ec load profile*

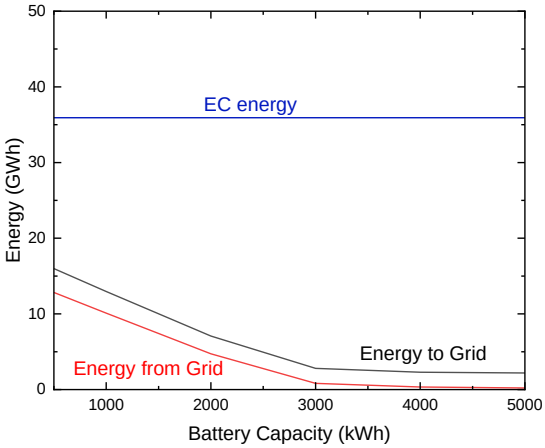

(c). *Hourly predicted Ec load profile*

Figure 3. 4. *Lifetime energy required as battery capacity varies for the Unpredicted, daily and hourly predicted EC load profile*

In the unpredicted case, it was observed that even with huge battery capacity of about 5MWh as compared to the system capacity of 1MW, the electrolyser still required significant amount of energy from the grid for full operation throughout its lifetime while in the Predicted daily, a reduction of the energy dispatched from the grid was observed but it was not very significant. However, in the hourly profile, significant improvement was observed as energy dispatched from the grid drop to zero with a 3MWh battery capacity. Excess energy that could be curtailed throughout the systems lifetime is also significantly reduced.

In the preceding graphs below (i.e., 3.5. (a) and (b)), the behaviour of the minimum operating power of the electrochemical device as it varies for the system and the required EC energy throughout the systems lifetime is presented for the predicted daily and hourly profile respectively. It is observed that the minimal power required by the EC contribute to the grid-exchange of the system and varies linearly with grid export and import.

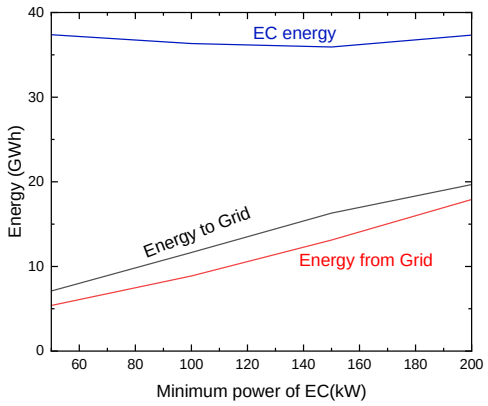

(a). *Daily predicted EC load profile*

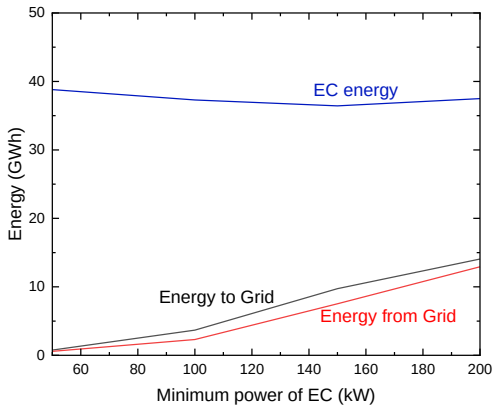

(b). *Hourly predicted EC load profile*

Figure 3.5. *Lifetime energy required as EC minimum power varies for the daily and hourly prediction*

In comparison, at the lower operating limit of 30% (i.e., 150kW), which is the assumed minimal operating point during the system optimization. It is observed that in both the daily and hourly prediction, the electrochemical-device total energy is approximately the same but the interaction with the grid is less in the hourly prediction.

3.4. Embodied Energy

The result obtained from the computation of the total energy required for the manufacturing and production phase of the inverter and nickel-cobalt maganese battery is presented in table 3.1. The results were compared with the values in the literature and it falls in the range as shown by reference of (Degen & Schütte, 2022; Prabhu et al., 2022; Tripathi & Subramanian, 2022). The table with the computed values are presented in the apendix. The datasets for the production and manufacturing of monocrystalline module and the BOS were collected from Triphati and Subramanien because in his analysis, the range of values available in the literature was given. However, the datasets were in MJ/m^2 so it was converted to kWh/m^2 for our analysis. Furthermore, the embodied energy for the alkaline water electrolyser obtained for our 1MW system is computed.

Table 3.1. *Components of the system and their total embodied energy for the construction and operation of the system*

Components	**Embedded Energy for production**	**Unit**
PV modules	1019	kWh/m2
Battery	39	kWh/kg
Inverter (size; 20kW)	58	kWh
AECs stack (for 1MW)	1,438,214	kWh
AECs BOP (for 1MW)	543,408	kWh
Array support, cabling and installation	37	kWh/m2

3.4.1. Embedded Energy of the Reference Case Configuration

Table 3.2. presents the computation of the required embedded energy in the reference-case system. From this table it is observed that, the PV- array is the most energy intensive in the process chain, which is consistent with the findings of (Palmer et al., 2021).

Table 3.2. *Total embodied energy in the reference-case configuration*

SYSTEM COMPONENTS	EMBEDDED ENERGY [MWh]
PV-array	5,108
AEC Stack	1,438
AEC BOP	543
Battery	424
Inverter	3
Array support, cabling & installation	173
Total	7,691

3.4.2. Embedded Energy of the Direct-Coupled Systems

For the direct coupled configuration, since the PV arrays voltage should match with the voltage of the electrolyser, sizing was based on the current state of the art architectures of alkaline electrolysers. According to (Frank et al., 2022)**,** alkaline electrolysers (AEC) stack voltages range from 18 to 522V, which gives the maximum operating voltage of an alkaline electrolysers which consist of 1 stack. So, in the design of the PV array, for a direct couple system. A 1MW capacity of electrolyser of 200 cells which totals to about 400V was considered. The resulted configuration of the system was 12 modules per string and 149 parallel strings.

3.4.2.1. Direct-Coupled PV-EC Configuration

Figure (3.6) shows a schematic representation of the direct coupled PV-EC without any power electronics.

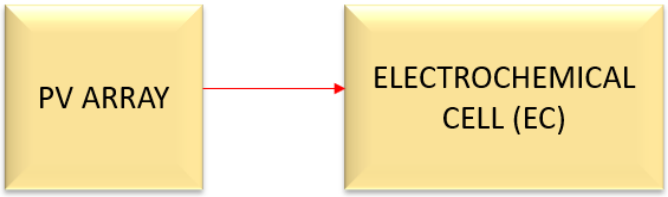

Figure 3.6. *Schematic representation of the direct coupled PV-EC configuration*

In this configuration, the embedded energy is less as compared with the reference case configuration (Table 3.3.) because of the absence of inverter and battery. Although, more cables are required in this configuration, but the contribution of the embedded energy of the battery is more significant.

Table 3.3. *Total embedded energy in the direct coupled PV-EC configuration*

SYSTEM COMPONENTS	EMBEDDED ENERGY [MWh]
PV-array	5,108
AEC Stack	1,438
AEC BOP	543
Array support, cable & installation	234
Total	7,324

3.4.2.2. Direct-Coupled PV-EV-B Configuration

Figure (3.7.) shows a schematic representation of the direct coupled PV-EC-B configuration. In this configuration, the battery acts as buffer and supply the electrochemical system when the PV generation is insufficient.

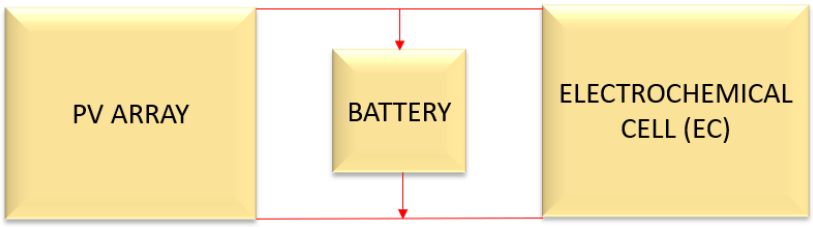

Figure 3.7. *Schematic representation of the direct coupled PV-EC-B configuration*

The embedded energy in this configuration (Table 3.4.) is less than the reference case scenario. However, the direct coupled PV-EC-B is more comparative to the reference case scenario because the main difference is the absence of the inverter.

Table 3.4. Total embedded energy in the direct coupled PV-EC-B configuration

SYSTEM COMPONENTS	**EMBEDDED ENERGY [MWh]**
PV-array	5,108
AEC Stack	1,438
AEC BOP	543
Battery	424
Array support, cabling & installation	94

Total	7,608

3.5. Comparisons of the Different Configurations

After optimization, the simulated results indicate a net energy generation from the system throughout its lifetime of 38 GWh, and a net energy generation without battery curtailment of 39 GWh. This indicates that in the case of the direct coupled PV-EC more energy can be generated from the PV-array as compared with the PV-EC-B, but due to the operational constraints of the electrolyser, and the coherent operation of the electrochemical cell with the PV generation in the direct coupled PV-EC, less hydrogen will be produced.

In this analysis, an AWE energy consumption of 51.63kWh/kg of H_2 is used, which is the average of the values in the literature as computed by (Tripathi & Subramanian, 2022). The hydrogen production was computed from the amount of energy supplied to the water electrochemical system (EC). And the energy payback time and EROI were computed. Table 3.5. present the net energy metric results of the different configurations.

Table 3.5. *System's total embedded energy, EPBT and EROI*

Systems	**Total embedded energy [MWh]**	**Energy Payback Time (EPBT) [Years]**	**Energy Return of Investment (EROI)**
PV-Inverter-EC-B	7691	10.57	2.36
Direct-coupled PV-EC	7324	10.06	2.48
Direct-coupled PV-EC-B	7608	10.46	2.39

The EROI values show the viability of the systems although is less than industrial requirement of 3:1. However, the values are comparable to the recent work of (Tripathi & Subramanian, 2022). In his analysis an EROI of 3.11 was obtain for the PV coupled with alkaline electrolyser, without a battery capacity and the total energy generation of the PV system was used for the computation of hydrogen production while in this analysis the amount of energy fed in the electrochemical cell is used for the EROI computation.

CONCLUSION AND PERSPECTIVES

With Hydrogen emerging as the most promising and versatile energy carrier that can utilize solar Photovoltaic energy to tackle climate change which result from the combustion of fossil fuels. Water electrolysis with the electrochemical water-splitting systems is the key towards this pathway. In this thesis, an analysis of the energetic performance of direct-coupled photovoltaic storage systems was performed to determine its long-term viability.

A quasi-island system was designed as the reference case for this analysis and the system was optimized. The optimization results indicate that, a significant battery capacity of 3MWh for a 1MW capacity is required, and the minimal power of the electrolyser is the key factor for system optimization. The net energy metric EROI evaluated indicate that the systems are viable options for green hydrogen production. With EROI of the battery assisted direct coupled photovoltaic electrochemical water splitting system higher than the battery assisted indirect-coupled photovoltaic-inverter-electrochemical water splitting system.

Future research work can broaden the scope of this analysis by extending the boundaries to point of use EROI, and adding the supplementary energy required for the transportation to the point of delivery. Also, different locations can be investigated, to determine how the energy performance metric varies. The main limitation of this research work is the unavailability of unit data of certain components in the process chain. Future research should attempt to compute all the amount of embedded energy required for the system and optimization of the direct couple configuration should be performed in order to perfectly depict the behaviour of the system.

REFERENCES

Araoz, F. B. (2021). *Lithium-ion batteries for off- -grid PV-systems. Doctoral thesis in Chemical engineering. KTH Royal institute of Technology: Stockholm, Sweden.*

Astakhov, O [O.], Agbo, S. N., Welter, K., Smirnov, V., Rau, U [U.], & Merdzhanova, T [T.] (2021). Storage batteries in photovoltaic–electrochemical device for solar hydrogen production. *Journal of Power Sources*, *509*, 230367. https://doi.org/10.1016/j.jpowsour.2021.230367

Barbera E, Mio A, Massi Pavan A, Bertucco A, & Fermeglia M. (2022). Sustainability Analysis of Hydrogen Production Processes: a Comparison Based on Sustainability Indicators, Chemical Engineering Transactions, 96, 109-114. DOI:10.3303/CET2296019

Behmann, R., Phan, J., Root, A., Schmidt, M., & Bessler, W. G. (2023). Integration of a lithium-ion battery in a micro-photovoltaic system: Passive versus active coupling architectures. *Solar Energy*, *262*, 111748. https://doi.org/10.1016/j.solener.2023.05.025

Bhandari, K. P., Collier, J. M., Ellingson, R. J., & Apul, D. S. (2015). Energy payback time (EPBT) and energy return on energy invested (EROI) of solar photovoltaic systems: A systematic review and meta-analysis. *Renewable and Sustainable Energy Reviews*, *47*, 133–141. https://doi.org/10.1016/j.rser.2015.02.057

Brauns, J., & Turek, T. (2020). Alkaline Water Electrolysis Powered by Renewable Energy: A Review. *Processes*, *8*(2), 248. https://doi.org/10.3390/pr8020248

Carbajales-Dale, M., Raugei, M., Fthenakis, V., & Barnhart, C. (Eds.) (2015). *Energy Return on Investment (EROI) of Solar PV: An Attempt at Reconciliation [Point of View]*. : Vol. *103*.

Davidsson Kurland, S., & Benson, S. M. (2019). The energetic implications of introducing lithium-ion batteries into distributed photovoltaic systems. *Sustainable Energy & Fuels*, *3*(5), 1182–1190. https://doi.org/10.1039/C9SE00127A

Degen, F., & Schütte, M. (2022). Life cycle assessment of the energy consumption and GHG emissions of state-of-the-art automotive battery cell production. *Journal of Cleaner Production*, *330*, 129798. https://doi.org/10.1016/j.jclepro.2021.129798

Dr Y (2021). British Colonial Treaties in Africa: The case of Banjul.

Dumas, J., Dubois, A., Thiran, P., Jacques, P., Contino, F., Cornélusse, B., & Limpens, G. (2022). The energy return on investment of whole energy systems: application to Belgium. *Biophysical Economics and Sustainability*, *7*(4), Article 12, 730. https://doi.org/10.1007/s41247-022-00106-0

Ehlers, J. C., Feidenhans'l, A. A., Therkildsen, K. T., & Larrazábal, G. O. (2023). Affordable Green Hydrogen from Alkaline Water Electrolysis: Key Research Needs from an Industrial Perspective. *ACS Energy Letters*, *8*(3), 1502–1509. https://doi.org/10.1021/acsenergylett.2c02897

ESMAP (2020). Global Photovoltaic Power potential by Country. Washington, DC: World Bank. Solargis: Country Factsheet, GMB.

FAO. (2005). AQUASTAT Country profile-Gambia. Food and Agriculture Organization of the United Nations (FAO). Rome, Italy.

Frank, G., Damien, G., Michel, Z., & and Hugues, R. (2022). A comprehensive survey of alkaline electrolyzer modeling: electrical domain and electrolyte conductivity, *15*(9). 10.3390/en15093452. hal-03663132

Fraunhofer Institute for Solar Energy Systems. (2023). *Photovoltaics Report.*

Gregor, E. (2023). EU rules for renewable hydrogen.

Gu, X., Ying, Z., Zheng, X., Dou, B., & Cui, G. (2023). Photovoltaic-based energy system coupled with energy storage for all-day stable PEM electrolytic hydrogen production, Article 209, 53–62.

Guangling Zhao, Mikkel Rykær Kraglund, Henrik Lund Frandsen, Anders Christian Wulff, Søren Højgaard Jensen, Ming Chen, & Christopher R. Graves (2020). Life cycle assessment of H2O electrolysis technologies.

Guerra-Martin, G. (2021). implementation-of-the-energy-return-on-investment-eroi-into-the-energyscope-td-model.

Gutiérrez-Martín, F., Amodio, L., & Pagano, M. (2021). Hydrogen production by water electrolysis and off-grid solar PV. *International Journal of Hydrogen Energy*, *46*(57), 29038–29048. https://doi.org/10.1016/j.ijhydene.2020.09.098

Gutiérrez-Martín, F., Díaz-López, J. A., Caravaca, A., & Dos Santos-García, A. J. (2023). Modeling and simulation of integrated solar PV - hydrogen systems. *International Journal of Hydrogen Energy.* Advance online publication. https://doi.org/10.1016/j.ijhydene.2023.05.179

International Renewable Energy Agency (IRENA). (2013). Renewables Readiness Assessment: The Gambia.

Kin, L.-C., Astakhov, O [Oleksandr], Lee, M., Haas, S., Ding, K., Merdzhanova, T [Tsvetelina], & Rau, U [Uwe] (2022). Batteries to Keep Solar-Driven Water Splitting Running at Night: Performance of a Directly Coupled System. *Solar RRL*, *6*(4), 2100916. https://doi.org/10.1002/solr.202100916

Koppelaar, R. (2017). Solar-PV energy payback and net energy: Meta-assessment of study quality, reproducibility, and results harmonization. *Renewable and Sustainable Energy Reviews*, *72*, 1241–1255. https://doi.org/10.1016/j.rser.2016.10.077

Kosol Kiatreungwattana, Otto VanGeet, and Blaise Stoltenberg: NREL. Facility-Scale Solar Photovoltaic Guidebook: Bureau of Reclamation.

M. Diesendorf, & T. Wiedmann (2020). Implications of Trends in Energy Return on Energy Invested (EROI) for Transitioning to Renewable Electricity.

Mark Ruth, Ahmad Mayyas, and Margaret Mann. Manufacturing Competitiveness Analysis for PEM and Alkaline Water Electrolysis Systems.

Megan, A. (2020). Designing a PV-Hydrogen-Battery-FC system for a typical neighbourhood in the Netherlands: Thesis.

Megía, P. J., Vizcaíno, A. J., Calles, J. A., & Carrero, A. (2021). Hydrogen Production Technologies: From Fossil Fuels toward Renewable Sources. A Mini Review. *Energy & Fuels*, *35*(20), 16403–16415. https://doi.org/10.1021/acs.energyfuels.1c02501

Müller, D., & Chartouni, D. (2022). Implications on EROI and climate change of introducing Li-ion batteries to residential PV systems. *Applied Energy*, *326*, 119958. https://doi.org/10.1016/j.apenergy.2022.119958

Nate Blair, Nicholas DiOrio, Janine Freeman, Paul Gilman, Steven Janzou, Ty Neises, and Michael Wagner. System Advisor Model (SAM) General Description (Version 2017.9.5).

Niroula, S., Chaudhary, C., Subedi, A., & Thapa, B. S. (2023). Parametric Modelling and Optimization of Alkaline Electrolyzer for the Production of Green Hydrogen. *IOP*

Conference Series: Materials Science and Engineering, *1279*(1), 12005. https://doi.org/10.1088/1757-899X/1279/1/012005

Nkanga, E. R. E., Ndoh, D. Z. N., Ntonda, J. N., Nanfak, A., Mekouebe, M. T., & Lontsi, F. (2021). Modeling of Hydrogen Production in an Alkaline Electrolyser System Connected with a Solar Photovoltaic Panel or a Wind Turbine: Case Study; Douala-Cameroon. *Journal of Power and Energy Engineering*, *09*(10), 1–18. https://doi.org/10.4236/jpee.2021.910001

Pahud, K., & Temmerman, G. de (2022). Overview of the EROI, a tool to measure energy availability through the energy transition. In *2022 8th International Youth Conference on Energy (IYCE)* (pp. 1–14). IEEE. https://doi.org/10.1109/IYCE54153.2022.9857542

Palmer, G., Roberts, A., Hoadley, A., Dargaville, R., & Honnery, D. (2021). Life-cycle greenhouse gas emissions and net energy assessment of large-scale hydrogen production via electrolysis and solar PV. *Energy & Environmental Science*, *14*(10), 5113–5131. https://doi.org/10.1039/D1EE01288F

Prabhu, V. S., Shrivastava, S., & Mukhopadhyay, K. (2022). Life Cycle Assessment of Solar Photovoltaic in India: A Circular Economy Approach. *Circular Economy and Sustainability*, *2*(2), 507–534. https://doi.org/10.1007/s43615-021-00101-5

Schoehuijs, T. (2018). Direct Coupling Feasibility Evaluation: Predicting the Price of Hydrogen Produced by Solar Energy. Master thesis. Delft University of Technology

Sharma, A. K., Pachauri, R. K., Choudhury, S., Minai, A. F., Alotaibi, M. A., Malik, H., & Márquez, F. P. G. (2023). Role of Metaheuristic Approaches for Implementation of Integrated MPPT-PV Systems: A Comprehensive Study. *Mathematics*, *11*(2), 269. https://doi.org/10.3390/math11020269

Shcherbachenko, S., Astakhov, O [Oleksandr], Chime, U., Kin, L.-C., Ding, K., Pieters, B., Rau, U [Uwe], Figgemeier, E., & Merdzhanova, T [Tsvetelina] (2023). Efficient Power Coupling in Directly Connected Photovoltaic-Battery Module. *Solar RRL*, *7*(3), 2200857. https://doi.org/10.1002/solr.202200857

Shriyan, N. R. (2020). Modelling of PV-Electrolyser system for optimum operation: Analysing the effect of variying irradiance, module parameters and comparison of various configurations for best efficiency. Master's thesis. Shell International Solutions BV, Amsterdam.

Tripathi, A. K., & Subramanian, K. A. (2022). Comparative life cycle energy and GHG emissions assessment of green hydrogen production with different electrolysers and solar photovoltaics system. In *2022 IEEE North Karnataka Subsection Flagship International Conference (NKCon)* (pp. 1–9). IEEE. https://doi.org/10.1109/NKCon56289.2022.10127022

Umair, S., & IEEE (2023). Analysis of Solar System Models Using System Advisor Model Simulations(9), Article 31, 23–32. https://www.researchgate.net/publication/363700701

Vega-Garita, V., Ramirez-Elizondo, L., Mouli, G. R. C., & Bauer, P. (2016). Review of residential PV-storage architectures, 1–6. https://doi.org/10.1109/ENERGYCON.2016.7514039

Wei, D., Li, H., Ren, Y., Yao, X., Wang, L., & Jin, K. (2022). Modeling of hydrogen production system for photovoltaic power generation and capacity optimization of energy storage system. *Frontiers in Energy Research, 10,* Article 1004277. https://doi.org/10.3389/fenrg.2022.1004277

World Bank. (2020). Systematic Country Diagnostic for the Republic of The Gambia: Overcoming a No-Growth Legacy. Washington, DC: World Bank.

Xia, Y., Cheng, H., He, H., & Wei, W. (2023). Efficiency and consistency enhancement for alkaline electrolyzers driven by renewable energy sources. *Communications Engineering*, *2*(1). https://doi.org/10.1038/s44172-023-00070-7

Xiong, & Nour (2019). Techno-Economic Analysis of a Residential PV-Storage Model in a Distribution Network. *Energies, 12*(16), 3062. https://doi.org/10.3390/en12163062

Module datasheet

Vertex BACKSHEET MONOCRYSTALLINE MODULE

DIMENSIONS OF PV MODULE(mm)

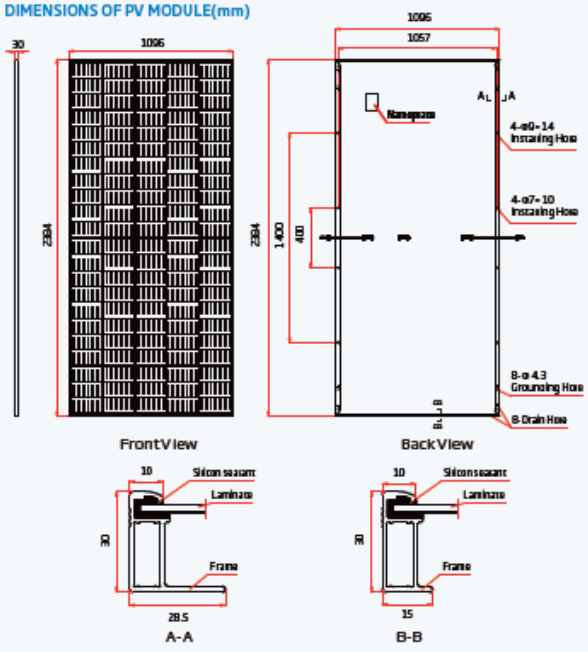

I-V CURVES OF PV MODULE(550 W)

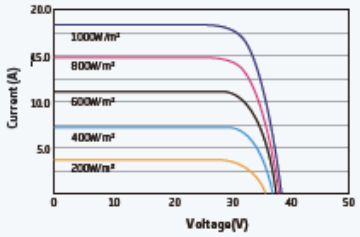

P-V CURVES OF PV MODULE(550W)

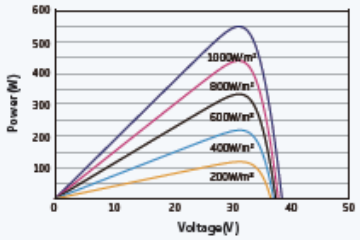

ELECTRICAL DATA (STC)

Peak Power Watts-PMAX (Wp)*	540	545	550	555	560
Power Tolerance-PMAX (W)			0~+5		
Maximum Power Voltage-VMPP (V)	31.2	31.4	31.6	31.8	32.0
Maximum Power Current-IMPP (A)	17.33	17.37	17.40	17.45	17.49
Open Circuit Voltage-Voc (V)	37.5	37.7	37.9	38.1	38.3
Short Circuit Current-Isc (A)	18.41	18.47	18.52	18.56	18.60
Module Efficiency η m (%)	20.7	20.9	21.0	21.2	21.4

STC: Irradiance 1,000W/m², Cell Temperature 25°C, Air Mass AM1.5. *Measuring tolerance: ±3%.

ELECTRICAL DATA (NOCT)

Maximum Power-PMAX (Wp)	409	413	417	420	424
Maximum Power Voltage-VMPP (V)	29.0	29.2	29.3	29.5	29.7
Maximum Power Current-IMPP (A)	14.10	14.15	14.19	14.23	14.26
Open Circuit Voltage-Voc (V)	35.3	35.5	35.7	35.9	36.1
Short Circuit Current-Isc (A)	14.84	14.88	14.92	14.96	14.99

NOCT: Irradiance at 800W/m², Ambient Temperature 20°C, Wind Speed 1m/s.

MECHANICAL DATA

Solar Cells	Monocrystalline
No. of cells	110 cells
Module Dimensions	2384×1096×30 mm (93.86×43.15×1.18 inches)
Weight	28.3 kg (62.39 lb)
Glass	3.2 mm (0.13 inches), High Transmission, Tempered Glass
Encapsulant material	EVA/POE
Backsheet	White
Frame	30 mm(1.18 inches) Anodized Aluminium Alloy
J-Box	IP 68 rated
Cables	Photovoltaic Technology Cable 4.0 mm² (0.006 inches²) Portrait: 350/280 mm(13.78/11.02 inches) Length can be customized
Connector	MC4-EVO2 / TS4 Plus / TS4*

*Please refer to regional datasheet for specified connector.

TEMPERATURE RATINGS

NOCT(Nominal Operating Cell Temperature)	43°C (±2°C)
Temperature Coefficient of PMAX	- 0.349%/°C
Temperature Coefficient of Voc	- 0.25%/°C
Temperature Coefficient of Isc	0.04%/°C

MAXIMUM RATINGS

Operational Temperature	-40~+85°C
Maximum System Voltage	1500V DC (IEC)
	1500V DC (UL)
Max Series Fuse Rating	30A

WARRANTY

12 year Product Workmanship Warranty

25 year Power Warranty

2% first year degradation

0.55% Annual Power Attenuation

(Please refer to product warranty for details)

PACKAGING CONFIGUREATION

Modules per box: 36pieces

Modules per 40' container: 720 pieces

Trinasolar

CAUTION: READ SAFETY AND INSTALLATION INSTRUCTIONS BEFORE USING THE PRODUCT.

Version number: TSM_EN_2023_A

www.trinasolar.com

Input values and result computation from SAM

System Advisor Model Report

Detailed Photovoltaic - Battery | 1.0 DC MW Nameplate | 13.57, -15.58
Commercial | $2.26/W Installed Cost | UTC +0

PV Performance Model

Modules	
User-specified parameters	
Cell material	monoSi
Module area	2.61 m²
Module capacity	559.68 DC Watts
Quantity	1,794
Total capacity	1 DC MW
Total area	4,682 m²

Inverters	
INGETEAM POWER TECHNOLOGY S A : INGECON SU	
Unit capacity	1000 AC kW
Input voltage	524 - 740 VDC DC V
Quantity	1
Total capacity	1,000 AC kW
DC to AC Capacity Ratio	1.00
AC losses (%)	0.00

Array	
Strings	69
Modules per string	26
String Voc (DC V)	995.80
Tilt (deg from horizontal)	20.00
Azimuth (deg E of N)	180
Tracking	no
Backtracking	-
Self shading	no
Rotation limit (deg)	-
Shading	no
Snow	no
Soiling	yes
DC losses (%)	4.44

Performance Adjustments	
Availability/Curtailment	none
Degradation	none
Hourly or custom losses	none

Annual Results (in Year 1)	
GHI kWh/m²/day	5.66
POA kWh/m²/day	136.00
Net to inverter	1,731,000 DC kWh
Net to grid	1,624,000 AC kWh
Capacity factor	18.5
Performance ratio	0.76

Battery Model

Battery Specifications	
Battery capacity	2,083.27 kWh
Battery chemistry	Lithium ion
Battery dispatch option	Manual dispatch
Minimum state of charge	0.2
Maximum state of charge	0.9

Battery Charge and Discharge	
Battery Capacity	2,083.27 kWh
Battery bank voltage	500.4 V
Number of cells	180,839
Cells in series	139
Strings in parallel	1,301
Max discharge power (DC)	217.01 kW
Max charge power (DC)	199.99 kW
Max discharge power (AC)	208.33 kW
Max charge power (AC)	208.33 kW
Max discharge current (A)	433.67 A
Max charge current (A)	399.67 A

Battery Performance	
Roundtrip eff. (%)	90.83
Cycle conversion eff. (%)	90.83
Average cycle DoD	63.98
Number of cycles	9,700
Year 1 energy charged	547,600.42 kWh
Year 1 charged from PV	547,600.41 kWh
Year 1 charged from grid	0 kWh
Year 1 energy discharged	497,797.16 kWh

Embedded energy computation

Inverter size in Kw for Europe (RER)	Electricity consumption in kWh	Natural gas consumption in MJ
2.5	10.6	0.226
2.5		3.57
2.5		9.21
Total		13.006
To convert the natural gas consumption in kWh:	3.612777778	
Therefore, total embodied energy for 2.5kW inverter is:	14.21277778	

Inverter size in kW for Europe (RER)	Electricity consumption in kWh	Natural gas consumption in MJ
5	16.9	0.361
5		5.72
5		14.7
Total		20.781
To convert the natural gas consumption in kWh:	5.7725	
Therefore, total embodied energy for 5kW inverter is:	22.6725	using LCI data from (IEA PVPS, 2020) database.

Inverter size in kW for Europe (RER)	Electricity consumption in kWh	Natural gas consumption in MJ
10	27.1	0.579
10		9.17
10		23.6
Total		33.349
To convert the natural gas consumption in kWh:	9.263611111	
Therefore, total embodied energy for 10kW inverter is:	36.36361111	

Inverter size in kW for Europe (RER)	Electricity consumption in kWh	Natural gas consumption in MJ
20	43.4	0.928
20		14.7
20		37.9
Total		53.528
To convert the natural gas consumption in kWh:	14.86888889	

NCM Li-ion battery production process	Electricity consumption in kWh/kg	Natural gas consumption in MJ/kg
Nickel-cobalt-manganese Lithium-ion battery	0.0004	
Single cell of Lithium-ion	22.7	
Cathode lithium-ion battery NCM, at plant		45.8
Diesel burned in building machine (GLO)		3.43
Electricity high voltage production, at grid (ENTSO)	0.448	
Electricity medium voltage production, at grid (ENTSO)	1.02	
Electricity hydro-power at runoff river power plant (RER)	0.671	
Heat at hard coal (RER)		0.316
Heavy fuel oil burned in industrial furnace (RER)		0.205
Natural gas burned in industrial furnace (RER)		1.24
Natural gas high pressure at consumer (CH)		0.0158
Hard coal coke, at plant (RER)		0.623
Total	24.8394	51.6298
To obtain the total natural gas value in kWh/kg:	14.34161111	

This implies that the total amount of energy embedded in a Nickel-cobalt-manganese battery of 1kg is: 39.18101111 using LCI data from (IEA PVPS, 2020) database.

Therefore, total embodied energy for 20kW inverter is: 58.26888889 using LCI data from (IEA PVPS, 2020) database.